PCCP

Interplay of Molecular Dynamics and Radiative Decay of a TADF Emitter in a Glass-Forming Liquid

Journal:	*Physical Chemistry Chemical Physics*
Manuscript ID	CP-ART-11-2022-005138.R1
Article Type:	Paper
Date Submitted by the Author:	23-Dec-2022

Complete List of Authors:	Swartzfager, John; Penn State University, Chemistry Chen, Gary; Penn State University, Chemistry Francese, Tommaso; The University of Chicago, Galli, Giulia; University of Chicago, PME Asbury, John; Penn State University, Chemistry

Interplay of Molecular Dynamics and Radiative Decay of a TADF Emitter in a Glass-Forming Liquid

John R. Swartzfager,[1] Gary Chen,[1] Tommaso Francese,[2] Giulia Galli,[2,3,4] and John B. Asbury[1*]

1. Department of Chemistry, The Pennsylvania State University, University Park, PA 16802, USA.

2. Pritzker School of Molecular Engineering, University of Chicago, Chicago, IL 60637, USA.

3. Materials Science Division and Center for Molecular Engineering, Argonne National Laboratory, Lemont, IL 60439, USA

4. Department of Chemistry, University of Chicago, Chicago, IL 60637, USA

Abstract

We investigate the role of molecular dynamics in the luminescent properties of a prototypical thermally activated delayed fluorescence (TADF) emitter, NAI-DMAC, in solution using a combination of temperature dependent time-resolved photoluminescence and absorption spectroscopies. We use a glass forming liquid, 2-methylfuran, to introduce an abrupt change in the temperature dependent diffusion dynamics of the solvent and examine the influence this has on the emission intensity of NAI-DMAC molecules. Comparison of experiment with first principles molecular dynamics simulations reveals that the emission intensity of NAI-DMAC molecules follows the temperature-dependent self-diffusion dynamics of the solvent. A marked reduction of emission intensity is observed as the temperature decreases toward the glass transition because the rate at which NAI-DMAC molecules can access emissive molecular conformations is greatly reduced. Below the glass transition, the diffusion dynamics of the solvent changes more slowly with temperature, which causes the emission intensity to decrease more slowly as well. The combination of experiment and computation suggests a pathway by which TADF emitters may transiently access a distribution of conformational states and avoid the need for an average conformation that strikes a balance between lower singlet-triplet energy splittings versus higher emission probabilities.

Introduction

Thermally activated delayed fluorescence (TADF) is a process by which organic emitters in organic light emitting devices (OLEDs) can utilize all four spin combinations resulting from the recombination of randomly spin-oriented electrons and holes. This is made possible because the excited triplet states of TADF emitters are close in energy to their singlet excited states.[1-5] Emitters in OLED systems that utilize TADF offer the opportunity to overcome the efficiency and sustainability issues of first- and second-generation OLEDs by allowing all-organic emitters to be used while still enabling high efficiencies by harvesting all four spin combinations.[6-11] The identification of such emitters relies on the development of design rules about how molecular structure influences the triplet excited states of molecules such that the

exchange interaction of excited states can be minimized, leading to singlet-triplet energy splittings small enough to allow triplet states to transition back into singlet excited states via reverse intersystem crossing.[12-14] Such processes are frequently thermally activated, although a recent report suggests this might not be the case for certain structures.[15]

Recent computational efforts have led to new understanding of the mechanisms underlying the TADF process and have provided insight about how the conformations of molecules influences their singlet-triplet energy splitting, oscillator strength, and spin-orbit coupling.[16-20] These computational efforts revealed that molecular conformations leading to the lowest singlet-triplet energy splittings involve nearly orthogonal dihedral angles between the donor and acceptor moieties of the molecules. Such geometries facilitate separation of the highest occupied molecular orbitals (HOMO) from lowest unoccupied molecular orbitals (LUMO). However, these nearly orthogonal dihedral angles also lead to states with low spin-orbit coupling and small transition dipole moments for radiative relaxation of their excited S_1 to ground S_0 states. Furthermore, density functional theory (DFT) and first principles molecular dynamics (MD) simulations of the prototypical TADF emitter examined in this work, NAI-DMAC[17, 20], revealed that a similar distribution of nearly orthogonal dihedral angles exists at room temperature in both isolated and crystalline NAI-DMAC molecules (structure depicted in **Figure 1A**).[17] **Figure 1B** represents the probability density of dihedral angles of isolated molecules at 300 K that were reported recently in Reference 17, employing first-principles MD with both a classical (CL) and a quantum thermostat (QT) to mimic nuclear quantum effects. Represented below the probability density are the variation (at T=0 K for simplicity) of the singlet-triplet energy splittings (ΔE_{ST}, **Figure 1C**) and the oscillator strength for the S_1 to S_0 radiative transition (f_{OS}, **Figure 1D**) that is related to the square of the transition dipole moment.[17] These molecular properties are plotted on the same dihedral angle scale for comparison and reveal that NAI-DMAC molecules at room temperature can adopt a variety of molecular conformations with a range of singlet-triplet energy splittings, spin-orbit couplings, and oscillator strengths. Interestingly, the value of ΔE_{ST} is not only determined by the angle between the donor and acceptor moieties but also by other geometrical degrees of freedom of the

molecule (shown by the comparison between relaxed and unrelaxed structures in **Figure 1C**). However, the oscillator strength (f_{OS}, **Figure 1D**) is almost exclusively determined by the dihedral angle.

Recent *ab initio* and atomistic MD simulations of the TADF emitter, DMAC-TRZ (10-4(4-(4,6-Diphenyl-1,3,5-triazin-2-yl)phenyl)-9,9-dimethyl-9,10-dihydroacridine), in common host matrices such as mCPCN (9-(3-(9H-carbazol-9-yl)phenyl)-9H-carbazole-3-carbonitrile) revealed that the molecules adopt a similar distribution of donor-acceptor dihedral angles.[21-25] Similar to NAI-DMAC, it was found that the near orthogonal molecular conformations of DMAC-TRZ with lowest singlet-triplet energy splittings also exhibited low spin-orbit coupling, which was predicted to decrease the rate of reverse intersystem crossing needed to allow the TADF process to occur.[21-25] An essential state model was parametrized using *ab initio* calculations of DMAC-TRZ[23] and included anharmonic and nonadiabatic contributions of the vibrational and conformational motion of the molecule.[24] The model was used to describe the effects of dielectric disorder and time-dependent polarization of the local environment[22, 24] to reproduce time-dependent frequency shifts of emission spectra of DMAC-TRZ in a variety of matrixes.[25] Taken together, these observations affirm the suggestion that molecules capable of undergoing efficient TADF may adopt molecular conformations and local environments that balance the competing needs for low singlet-triplet energy splittings with high spin-orbit coupling and radiative relaxation probabilities.

To further explore this dependence on molecular conformation and local environment, we used time-resolved photoluminescence (TRPL) combined with UV-visible absorption spectroscopy to examine the emission characteristics of NAI-DMAC molecules in solution at a range of temperatures. Importantly, we used a glass forming liquid, 2-methylfuran (mTHF), that exhibits an abrupt change in its temperature dependent self-diffusion dynamics[26] to explore the influence the dynamics of the local environment have on the emission intensity of NAI-DMAC molecules. Our findings in conjunction with electronic structure and first principles MD simulations demonstrate that in solution it is the ability of NAI-DMAC molecules to transiently access conformations with higher oscillator strengths that leads to efficient radiative relaxation. Our findings suggest that TADF emitters in solution may be able to transiently access conformational states with low singlet-triplet energy splittings and then undergo conformational dynamics

with coordinated motion of the solvent to access states with greater transition dipole moments. TADF emitters capable of transiently accessing both types of conformational states in a serial fashion within their singlet excited state lifetimes have the potential to overcome the need to find molecular conformations that balance these properties. Future work in this direction will explore the role that molecular conformational motion and polarization of the local environment[24, 25] may play in the TADF process in solid matrices that are relevant to applications of TADF emitters in OLEDs.

Experimental Methods

Sample Preparation. NAI-DMAC was purchased from Lumtec and used without further purification. Solutions for photoluminescence measurements were made by dissolving NAI-DMAC in mTHF to form a solution with final concentration of 900μM. This concentration was used because the samples were placed into 1mm quartz cuvettes to enable rapid thermal equilibration during the temperature dependent measurements. The solutions were sparged by vigorously bubbling N_2 gas in the sealed and vented cuvette for a minimum of five minutes. The removal of O_2 in the solutions using this method was verified by comparison of the time-integrated PL intensities of samples sparged in this manner for 15 minutes as represented in **Figure S1**. The minute difference between these spectra is within experimental precision of the measurement.

UV-Visible Absorption Measurements. Absorption spectra were collected using a commercially available Beckman DU520 instrument. Reference spectra were collected using the pure solvent in an identical cuvette placed in the same optical geometry as the sample.

Temperature Dependent UV-Visible Absorption Measurements. Temperature dependent absorption spectra were performed using an enVISion transient absorption spectrometer (Magnitude Instruments, State College, PA) with the pump source blocked. A Xenon lamp was used as the probe source, the light from which was focused onto the sample and then collected by lenses and focused through the slits of a monochromator before being detected by an avalanche photodiode. During the experiments, the sealed

cuvettes were placed in an evacuated, liquid N_2 cooled cryostat (ST-100, JANIS Research, Woburn, MA) under high vacuum to allow control of the temperature using a Lakeshore 331 temperature controller (Carson, CA).

Time-resolved Photoluminescence Measurements. Nanosecond TRPL spectroscopy was performed using an enVISion transient absorption spectrometer (Magnitude Instruments, State College, PA) with the probe source blocked. A Continuum Surelite 30Hz, 10ns Nd:YAG laser (San Jose, CA) with a 355 nm output and 65 $\mu J/cm^2$ intensity was used as the excitation source. The emission from the sample was collected by lenses, at a 90° angle relative to the excitation source, and focused through the slits of a monochromator before being detected by a silicon photodiode. During the experiments, the samples in sealed cuvettes were placed in an evacuated, liquid N_2 cooled cryostat (ST-100, JANIS Research, Woburn, MA) under high vacuum to allow control of the temperature using a Lakeshore 331 temperature controller (Carson, CA). The sample was stabilized at each desired temperature and held at that temperature for ten minutes to ensure thermal equilibrium had been established prior to collection of the transient spectra and kinetics. After this, the next temperature was selected, and the stabilization and equilibration procedures were repeated prior to the next TRPL measurement. The placement of the sealed cuvettes under high vacuum during the measurements insured no air exchange or introduction of O_2 during the measurements.

Results and Discussion

In this work, we investigated the role that dynamic interconversion of molecular conformations has on the emissive properties of NAI-DMAC using temperature dependent TRPL and UV-visible absorption spectroscopy studies in solution. NAI-DMAC consists of an electron donating 9,9-dimethyl-9,10-dihydroacridine (DMAC) unit bonded to an electron accepting N-(4-tert-butylphenyl)-1,8-naphthalimide (NAI) unit.[17, 20] The NAI and DMAC units are able to rotate around the dihedral bond which connects them. It is this dihedral bond that gives NAI–DMAC the ability to take on a twisted geometry, which is characteristic of many TADF emitters.[1, 27]

The electronic absorption spectra of NAI-DMAC in toluene, mTHF, and chloroform are represented as solid curves in **Figure 2**. The spectra exhibit two prominent features at 350 and 470 nm. The transition at 350 nm has been assigned to a π-π* transition localized to the NAI unit of the molecule.[20] The peak at approximately 470 nm has been assigned to an n-π* transition involving the DMAC nitrogen lone pair because it is believed to be weekly conjugated to the NAI unit,[28] suggesting the transition may have intramolecular charge transfer character. The steady-state PL spectra of NAI-DMAC in toluene, mTHF, and chloroform are represented in **Figure 2** as the dashed curves. The spectra exhibit a systematic shift to longer emission wavelength with increasing polarity, which is consistent with an intramolecular charge transfer state. The red shift with increasing polarity is due to the ability of more polar solvents to stabilize the charge transfer character of the excited state, while destabilizing the ground state.[29-33] It has been shown in numerous other works that emission in TADF compounds commonly occurs from intramolecular charge transfer states.[8, 28, 34-37]

The DFT and first principles MD computations of isolated NAI-DMAC molecules summarized in **Figure 1**[17] demonstrate that the energies of the singlet and triplet electronic states depend sensitively on their molecular geometry. Similar to prior work on DMAC-TRZ,[21-25] the first principles MD simulations revealed that NAI-DMAC molecules are most likely to be found in configurations with nearly orthogonal dihedral angles where the singlet-triplet energy splittings are smallest. Prior studies of related TADF emitters revealed aggregation induced emission, wherein the assembly of molecules in a solid film restricts their conformational motion and slows access to non-radiative relaxation pathways, leading to higher emission quantum yields in the solid state.[38-41] Interestingly, both isolated NAI-DMAC molecules at 300K and DMAC-TRZ suspended in a mCPCN matrix show similar distributions of the dihedral angle between the donor and acceptor moieties of the molecule, with values ranging from 60° to 120° with an average of ~90°.[17, 21]

We note that the comparison of the unrelaxed versus relaxed computational results in **Figure 1C** reveal that the singlet-triplet energy splitting values depend sensitively on other nuclear coordinates in addition to the dihedral angle.[17] In the relaxed computations, other nuclear coordinates were allowed to

vary to minimize total energy at each fixed dihedral angle. This optimization step was not completed for the unrelaxed computations. In contrast, **Figure 1D** revealed that molecules in these most probable nuclear configurations also have lowest probability for radiative decay due to their low oscillator strengths and low spin orbit couplings.[17] Importantly, the comparison of the unrelaxed and relaxed computational results revealed that the oscillator strength of NAI-DMAC molecules depends almost exclusively on the dihedral angle. These findings demonstrated that NAI-DMAC molecules must distort from their nearly orthogonal dihedral structure to have a high probability for radiative decay, which also increased their singlet-triplet energy splitting and spin orbit coupling.[17]

We hypothesized on the basis of these computational studies that dynamic conformational motion may figure prominently in the radiative decay process of TADF emitters because TADF molecules with more twisted molecular geometries have smaller singlet-triplet energy splittings but also smaller transition dipole moments. To test this hypothesis, we examined the effect of temperature on the electronic absorption spectra and TRPL decay properties of NAI-DMAC dissolved in mTHF. mTHF is a glass forming liquid that preserves its liquid structural disorder over a wide temperature range but exhibits an abrupt change in its temperature dependent self-diffusion coefficient near its glass transition temperature.[26, 42, 43] We prepared solutions of NAI-DMAC in mTHF with 0.9 millimole/L concentration and varied their temperature from 300 K to 80 K, which spans the 130 - 140 K glass transition temperature of mTHF.[26] We reasoned that temperature dependent solution studies would provide a way to systematically tune the time scale on which NAI-DMAC molecules could undergo dynamic conformational motion within their excited singlet and triplet state lifetimes.

If NAI-DMAC molecules rely on dynamic access to molecular conformations with stronger transition dipole moments and spin orbit coupling to enable the TADF process, then we should expect the emission quantum yields of TADF emitters in solution to vary significantly with temperature. This is because the reduction of thermal energy should slow the rate at which the surrounding mTHF molecules can accommodate dynamic conformational motion of NAI-DMAC and reduce the rate at which they can transiently access highly emissive geometries. This effect should be particularly pronounced as mTHF cools

and approaches its glass transition temperature because the self-diffusion dynamics of the solvent slow rapidly with small changes of temperature near this transition.[26] However, if transient access to certain molecular conformations is not an important determining factor for the radiative relaxation rate of TADF emitters, then we should expect such molecules to exhibit relatively little dependence of their emission quantum yields versus temperature, similar to observations of TADF emitters in the solid state.[44, 45]

We first verified that the distribution of conformational states of NAI-DMAC molecules in mTHF exhibited little change with temperature by measuring the electronic absorption spectra of the NAI-DMAC solution over the 300 K to 80 K temperature range. **Figure 3A** depicts the absorption spectra spanning both the π-π* and the n-π* transitions. The π-π* transitions exhibit small changes in oscillator strength but negligible changes in width over the temperature range. The inset is focused on the lower amplitude n-π* transition where the spectra are normalized to facilitate comparison of the widths of the transition as a function of temperature. Because the energies of the singlet electronic states depend on conformation,[17] we reasoned that changes in the width and central wavelength of the π-π* and the n-π* transitions would indicate that the distribution of conformational states of NAI-DMAC molecules changed with temperature. The apparent invariance of both the width and central wavelength of the transitions in **Figure 3A** suggests that the distribution of conformational states of NAI-DMAC molecules are comparable across the full range of temperatures examined here.[46-48]

We then examined the temperature dependence of the steady-state PL spectra of NAI-DMAC in mTHF solution to evaluate the influence that changes in available thermal energy have on the ability of NAI-DMAC molecules to undergo radiative relaxation. **Figure 3B** represents unnormalized time-integrated PL spectra of NAI-DMAC in mTHF following optical excitation at 355 nm and measured at a range of temperatures from 300 K to 80 K. While the unnormalized absorption spectra of the samples changed little with temperature, the temperature dependent PL spectra exhibit a factor of 10 reduction of amplitude as the temperature decreased. Such a reduction of PL amplitude cannot be explained by the small variation of absorbance of the samples at the pump wavelength because their absorption increased slightly at lower temperature, which is counter to the observed trend. Furthermore, changes in the self-absorption of the PL

cannot be the cause of the reduction at lower temperature because the samples absorb only weakly in the spectral range where the PL is emitted (**Figure 3A**).

We note that the temperature dependent changes of PL intensities appearing in **Figure 3B** may include a small contribution from the influence temperature has on the refractive index of the mTHF solution and quartz cuvette. For example, the optical geometry of the TRPL instrument utilized an F-number of seven for the condenser lens, which had a modest cone angle of four degrees for coupling emission from the sample into the detection system. We estimate from the maximum angle of incidence of light leaving the cuvette and successfully entering the condenser lens that a 10% reduction of the refractive index of mTHF with decreasing temperature would result in at most a 20% increase of the measured PL intensity. This is because a slightly larger cone angle of the emitted light would be captured by the detection system due to the change in refraction angle between the solvent and the quartz wall of the cuvette. A 20% increase in intensity with decreasing temperature is counter to the ten-fold reduction of intensity that we observe, which is dominated by the changes in molecular dynamics of mTHF and their influence on the emissive properties of NAI-DMAC over the range of temperatures examined here.

Figure 3C displays unnormalized TRPL emission kinetics measured of NAI-DMAC in mTHF solution at a range of temperatures. The kinetics also exhibit marked reduction in intensity at lower temperatures with little change in shape, indicating that the temperature-dependent effects determining the emission intensity occurred on the few nanosecond time scale. This marked reduction of PL intensity at lower temperature is counter to common temperature dependent emission behaviors that typically exhibit increased PL intensity at lower temperatures.[49-52] Such typical behavior arises from thermal occupation of low frequency vibrational modes that allow access to non-radiative relaxation pathways such as conical intersections, leading to lower intensity emission at elevated temperatures.[50, 53]

The observation here of lower PL intensity at lower temperature cannot be explained by this phonon-assisted non-radiative decay mechanism because it exhibits the opposite trend. Rather, the temperature dependence of the PL intensity indicates the need for NAI-DMAC molecules to reach states capable of undergoing radiative relaxation. Such behavior is consistent with computational predictions that

indicate NAI-DMAC molecules must reach conformations with dihedral twist angles that deviate significantly from the near-orthogonal geometries to access states with greater radiative decay probability (**Figure 1**).[17, 54, 55]

To further quantify the observed decrease in prompt emission with decreasing temperature we considered that the quantum yield of emission ϕ from NAI-DMAC molecules is related to the ratio of the radiative emission rate k_R to the sum of rates of all excited state decay paths. For simplicity, we describe the sum of all excited state decay paths as $k_R + k_{NR}$ in the quantum yield expression, $\phi = k_R / (k_R + k_{NR})$, where k_{NR} represents the sum of rates of all non-radiative decay processes.[56, 57] The need for NAI-DMAC molecules to access conformational states with less twisted dihedral angles to undergo emission suggests that the radiative decay rate k_R may depend on temperature because the diffusion dynamics of liquids vary with temperature.

We plotted in **Figure 4** the logarithm of the PL intensity from NAI-DMAC in mTHF *ln*(*Int*) versus inverse temperature 1/T in order to explore the correlation of the radiative decay process of NAI-DMAC molecules with the diffusion dynamics of the solvent. The PL intensities at each temperature were evaluated by integrating the emission spectra from 500 to 900 nm within the 8 – 12 ns time window. Therefore, the PL intensities correspond to the prompt emission component from NAI-DMAC molecules. The plot of the logarithm of intensity versus the inverse temperature exhibits behavior mimicking the temperature dependence of the self-diffusion coefficient of mTHF obtained from MD simulations reported in Reference 26 including the knee around the glass transition temperature.

To rationalize the correlation of the PL intensity of NAI-DMAC with mTHF diffusion dynamics, we note that the measurements at 300, 250, and 200 K (shaded box in **Figure 4**) are all above the glass transition temperature of mTHF. Within this range, the self-diffusion coefficient of mTHF varies by nearly three orders of magnitude[26] as the reduction of thermal energy slows the diffusion dynamics of molecules in the liquid. Such motion may include solvent polarization effects.[24, 25] This large change of diffusion dynamics most strongly impacts the radiative decay rate k_R because of the need for molecules to undergo

conformational motion with associated motion of the solvent in order to access conformations with greater transition dipole moments.[17] We note that the change in thermal energy is modest over this range because the temperature decreased by only 33% relative to its initial value at 300 K. If the rate of non-radiative decay k_{NR} changed significantly with temperature due to changes in phonon-assisted relaxation processes, then the corresponding influence on the PL intensities would be opposite to the observed decrease with decreasing temperature.[49-52] While we cannot eliminate the possible influence of temperature dependent changes in non-radiative decay, we can conclude that the emissive properties of NAI-DMAC in solution are dominated by the molecular dynamics of the solvent and their influence on the structural dynamics of the emitter. Therefore, the slope of the line obtained from the $ln(Int)$ versus 1/T data in the 300 to 200 K range is dominated by the temperature dependence of diffusive motion of mTHF and its influence on k_R.

In the 150 to 80 K temperature range, a marked change of slope is observed, which corresponds with the change in slope of the temperature dependent self-diffusion coefficient of mTHF.[26] Within this temperature range, mTHF is already close to and then passes through its glass transition with a corresponding modest change in diffusion dynamics of only one order of magnitude.[26] There is a corresponding smaller reduction of the PL intensity associated with this lesser variation of the self-diffusion dynamics with temperature of the mTHF molecules. We recognize there may have been some change of the occupation of low frequency vibrational modes of NAI-DMAC moving from 150 K to 80 K, which could influence the rate of non-radiative decay k_{NR}. None the less, the temperature dependent intensity variation follows closely the changes in mTHF self-diffusion coefficient reported in Reference 26, again indicating that the emission probability of NAI-DMAC molecules is dominated by the molecular dynamics of the solvent and how they influence the structural motion of the emitter. This correlation indicates that radiative relaxation of NAI-DMAC molecules relies on their ability to transiently access conformational states with greater radiative relaxation rates, which requires motion of solvent molecules. As the temperature decreased, the NAI-DMAC molecules were less likely to reach their emissive configurations within the singlet excited state lifetime, leading to marked reduction of their emission intensity. Comparison

to computational results indicates these conformational states are those with smaller dihedral twist angles or more puckered geometries.[17]

Finally, it is useful to discuss how the temperature dependent changes in molecular dynamics of mTHF that influence the emissive properties of NAI-DMAC affect the dielectric properties of the solvent. This is because the principal contribution to the low frequency dielectric constant of dipolar liquids such as mTHF arises from the orientation of dipoles within the liquid.[58, 59] At room temperature, thermal energy is sufficient to overcome most of the dipole-dipole interactions, causing the molecular dynamics of the liquid to produce isotropic distributions of dipoles at room temperature. This leads to a modest dielectric constant of 7.5 of mTHF at 300 K.[60] However, at lower temperatures with reduced thermal energy available, the molecular dynamics of the liquid are insufficient to overcome dipole-dipole interactions. The stronger influence of dipole-dipole interactions in the liquid while the molecules are still able to undergo dynamic motion leads to greater screening of charge, which causes the significant increase of the dielectric constant at lower temperature.[61]

Therefore, the temperature dependent dielectric constant of a dipolar liquid is an important manifestation of the temperature dependence of the molecular dynamics in the liquid. It has been shown that translational motion of molecules, not just their orientational motion, must be included in molecular dynamics models of the dielectric properties of dipolar liquids.[62] This greater extent of molecular motion also allows faster and larger scale motion of solute molecules within the solvent, which in turn allows NAI-DMAC molecules to undergo conformational motion to transiently access structures with higher radiative relaxation probabilities within their excited state lifetime. It also leads to higher energy emission because of the reduced ability of solvent molecules to stabilize the dipole of the excited state as a result of thermally induced dipolar disorder, which is manifested in the shorter wavelength emission maximum of NAI-DMAC at 300 K (**Figure 3B**). At lower temperatures, the thermal motion of dipolar molecules is reduced, which allows dipole-dipole interactions between molecules to more strongly screen charge.[58, 59] This decrease of thermal motion of the solvent also restricts larger scale motion of solute molecules within the solvent, which reduces the probability that NAI-DMAC molecules in mTHF can transiently access their emissive

conformations within their excited state lifetime, leading to the reduction of their emission intensity at lower temperatures.

Conclusion

We used a combination of temperature-dependent time-resolved photoluminescence and optical absorbance spectroscopy to examine the emissive properties of a prototypical thermally activated delayed fluorescence emitter, NAI-DMAC, in solution. A glass forming liquid, 2-methylfuran (mTHF), was used as the solvent to introduce an abrupt change in the temperature dependence of the diffusion dynamics of the liquid so these could be correlated with the variation of the emission intensity of NAI-DMAC molecules. The variation of the photoluminescence intensity of NAI-DMAC in solution followed the temperature dependence of the self-diffusion coefficient of mTHF reported in the literature.[26] Comparison of the experimental findings to first-principles molecular dynamics simulations reveals that NAI-DMAC molecules must access conformational states with smaller twist angles and larger singlet-triplet energy splittings in order to undergo radiative decay in solution. The temperature dependent photoluminescence intensity measurements reveal that the rate at which NAI-DMAC molecules can reach such emissive states depends on the diffusion dynamics of the solvent, demonstrating that access to such states is an inherently dynamic not a static process in solution. Our findings suggest a pathway for molecules to undergo thermally activated delayed fluorescence in which molecules may experience reverse intersystem crossing while they reside in their more twisted conformations with lower singlet-triplet energy splitting values. Then, within their singlet excited state and intersystem crossing lifetimes, they may undergo conformational motion to access less twisted or more puckered conformations with greater emission probabilities. In future work, it will be interesting to investigate the potential role such intertwined excited state and molecular conformational dynamics may play in the TADF process of molecules in the solid state.

Author Information

Corresponding Author

J.B.A.: jasbury@psu.edu

Acknowledgments

The authors acknowledge financial support for this work from the Office of Naval Research (Program manager P. Armistead, award N00014-19-1-2453). We thank Prof. Enrique Gomez, Prof. Zhenan Bao, Prof. Scott Milner, Prof. Alberto Salleo, Dr. Paul Cunningham, and Dr. Lee Richter for many useful discussions.

DECLARATION OF INTERESTS

J. B. A. owns equity in Magnitude Instruments, which has an interest in this project. His ownership in this company has been reviewed by the Pennsylvania State University's Individual Conflict of Interest Committee and is currently being managed by the University.

References

1. Dias, F. B.; Penfold, T. J.; Monkman, A. P., Photophysics of thermally activated delayed fluorescence molecules. *Methods Appl. Fluoresc.* **2017,** *5*, 012001.
2. Delorme, R.; Perrin, F., Durées de fluorescence des sels d'uranyle solides et de leurs solutions. *J. Phys. Radium* **1929,** *10*, 177-186.
3. Lewis, G. N.; Lipkin, D.; Magel, T. T., Reversible Photochemical Processes in Rigid Media. A Study of the Phosphorescent State. *J. Am. Chem. Soc.* **1941,** *63*, 3005-3018.
4. Brown, R. E.; Singer, L. A.; Parks, J. H., Prompt and delayed fluorescence from benzophenone. *Chem. Phys. Lett.* **1972,** *14*, 193-195.
5. Endo, A.; Sato, K.; Yoshimura, K.; Kai, T.; Kawada, A.; Miyazaki, H.; Adachi, C., Efficient up-conversion of triplet excitons into a singlet state and its application for organic light emitting diodes. *Appl. Phys. Lett.* **2011,** *98*, 083302.
6. Liu, Y.; Li, C.; Ren, Z.; Yan, S.; Bryce, M. R., All-organic thermally activated delayed fluorescence materials for organic light-emitting diodes. *Nat. Rev. Mater.* **2018,** *3*, 18020.
7. Noda, H.; Nakanotani, H.; Adachi, C., Excited state engineering for efficient reverse intersystem crossing. *Sci. Adv.* **2018,** *4*, eaao6910.
8. Zhang, Q.; Li, B.; Huang, S.; Nomura, H.; Tanaka, H.; Adachi, C., Efficient blue organic light-emitting diodes employing thermally activated delayed fluorescence. *Nat. Photon.* **2014,** *8*, 326-332.
9. Penfold, T. J., On Predicting the Excited-State Properties of Thermally Activated Delayed Fluorescence Emitters. *J. Phys. Chem. C* **2015,** *119*, 13535-13544.

10. Tao, Y.; Yuan, K.; Chen, T.; Xu, P.; Li, H.; Chen, R.; Zheng, C.; Zhang, L.; Huang, W., Thermally Activated Delayed Fluorescence Materials Towards the Breakthrough of Organoelectronics. *Adv. Mater.* **2014,** *26*, 7931-7958.
11. Adachi, C., Third-generation organic electroluminescence materials. *Jpn. J. Appl. Phys.* **2014,** *53*, 060101.
12. Gibson, J.; Penfold, T. J., Nonadiabatic coupling reduces the activation energy in thermally activated delayed fluorescence. *Phys. Chem. Chem. Phys.* **2017,** *19*, 8428-8434.
13. Wong, M. Y.; Zysman-Colman, E., Purely Organic Thermally Activated Delayed Fluorescence Materials for Organic Light-Emitting Diodes. *Adv. Mater.* **2017,** *29*, 1605444.
14. Kim, C. A.; Van Voorhis, T., Maximizing TADF via Conformational Optimization. *J. Phys. Chem. A* **2021,** *125*, 7644-7654.
15. Aizawa, H.; Pu, Y.-J.; Harabuchi, Y.; Nihonyanagi, A.; Ibuka, R.; Inuzuka, H.; Dhara, B.; Koyama, Y.; Nakayama, K.-i.; Maeda, S.; Araoka, F.; Miyajima, D., Delayed Fluorescence from Inverted Singlet and Triplet Excited States. *Nature* **2022,** *609*, 502-506.
16. Northey, T.; Stacey, J.; Penfold, T. J., The role of solid state solvation on the charge transfer state of a thermally activated delayed fluorescence emitter. *J. Mater. Chem. C* **2017,** *5*, 11001-11009.
17. Francese, T.; Kundu, A.; Gygi, F.; Galli, G., Quantum simulations of thermally activated delayed fluorescence in an all-organic emitter. *Phys. Chem. Chem. Phys.* **2022,** *24*, 10101-10113.
18. Chen, X.-K.; Kim, D.; Brédas, J.-L., Thermally Activated Delayed Fluorescence (TADF) Path toward Efficient Electroluminescence in Purely Organic Materials: Molecular Level Insight. *Acc. Chem. Res.* **2018,** *51*, 2215-2224.
19. Bas, E. E.; Ulukan, P.; Monari, A.; Aviyente, V.; Catak, S., Photophysical Properties of Benzophenone-Based TADF Emitters in Relation to Their Molecular Structure. *J.Phys. Chem. A* **2022,** *126*, 473-484.
20. Zeng, W.; Lai, H.-Y.; Lee, W.-K.; Jiao, M.; Shiu, Y.-J.; Zhong, C.; Gong, S.; Zhou, T.; Xie, G.; Sarma, M.; Wong, K.-T.; Wu, C.-C.; Yang, C., Achieving Nearly 30% External Quantum Efficiency for Orange–Red Organic Light Emitting Diodes by Employing Thermally Activated Delayed Fluorescence Emitters Composed of 1,8-Naphthalimide-Acridine Hybrids. *Adv. Mater.* **2018,** *30*, 1704961.
21. Hu, T.; Han, G.; Tu, Z.; Duan, R.; Yi, Y., Origin of High Efficiencies for Thermally Activated Delayed Fluorescence Organic Light-Emitting Diodes: Atomistic Insight into Molecular Orientation and Torsional Disorder. *J. Phys. Chem. C* **2018,** *122*, 27191-27197.
22. Phan Huu, D. K. A.; Dhali, R.; Pieroni, C.; Di Maiolo, F.; Sissa, C.; Terenziani, F.; Painelli, A., Antiadiabatic View of Fast Environmental Effects on Optical Spectra. *Phys. Rev. Lett.* **2020,** *124*, 107401.
23. Dhali, M.; Phan Huu, D. K. A.; Bertocchi, F.; Sissa, C.; Terenziani, F.; Painelli, A., Understanding TADF: a joint experimental and theoretical study of DMAC-TRZ. *Phys. Chem. Chem. Phys.* **2021,** *23*, 378-387.
24. Phan Huu, R.; Saseendran, R.; Painelli, A., Effective Models for TADF: the role of the medium polarizability. *J. Mater. Chem. C* **2022,** *10*, 4620-4628.
25. Phan Huu, D. K. A.; Saseendran, S.; Dhali, R.; Franca, L. G.; Stavrou, K.; Monkman, A. P.; Painelli, A., Thermally Activated Delayed Fluorescence: Polarity, Rigidity, and Disorder in Condensed Phases. *J. Am. Chem. Soc.* **2022,** *144*, 15211-15222.
26. Tan, R.-R.; Shen, X.; Hu, L.; Zhang, F.-S., Liquid-to-glass transition of tetrahydrofuran and 2-methyltetrahydrofuran. *Chin. Phys. B* **2012,** *21*, 086402.
27. Liang, X.; Tu, Z.-L.; Zheng, Y.-X., Thermally Activated Delayed Fluorescence Materials: Towards Realization of High Efficiency through Strategic Small Molecular Design. *Chem. Eur. J.* **2019,** *25*, 5623-5642.
28. Stavrou, K.; Franca, L. G.; Monkman, A. P., Photophysics of TADF Guest–Host Systems: Introducing the Idea of Hosting Potential. *ACS Appl. Electron. Mater.* **2020,** *2*, 2868-2881.

29. dos Santos, P. L.; Ward, J. S.; Batsanov, A. S.; Bryce, M. R.; Monkman, A. P., Optical and Polarity Control of Donor–Acceptor Conformation and Their Charge-Transfer States in Thermally Activated Delayed-Fluorescence Molecules. *J. Phys. Chem. C* **2017,** *121*, 16462-16469.
30. dos Santos, P. L.; Ward, J. S.; Bryce, M. R.; Monkman, A. P., Using Guest–Host Interactions To Optimize the Efficiency of TADF OLEDs. *J. Phys. Chem. Lett.* **2016,** *7*, 3341-3346.
31. Niu, X.; Gautam, P.; Kuang, Z.; Yu, C. P.; Guo, Y.; Song, H.; Guo, Q.; Chan, J. M. W.; Xia, A., Intramolecular charge transfer and solvation dynamics of push–pull dyes with different π-conjugated linkers. *Phys. Chem. Chem. Phys.* **2019,** *21*, 17323-17331.
32. Pasman, P.; Rob, F.; Verhoeven, J. W., Intramolecular charge-transfer absorption and emission resulting from through-bond interaction in bichromophoric molecules. *J. Am. Chem. Soc.* **1982,** *104*, 5127-5133.
33. Legaspi, C. M.; Stubbs, R. E.; Wahadoszaman, M.; Yaron, D. J.; Peteanu, L. A.; Kemboi, A.; Fossum, E.; Lu, Y.; Zheng, Q.; Rothberg, L. J., Rigidity and Polarity Effects on the Electronic Properties of Two Deep Blue Delayed Fluorescence Emitters. *J. Phys. Chem. C* **2018,** *122*, 11961-11972.
34. Dias, F. B.; Bourdakos, K. N.; Jankus, V.; Moss, K. C.; Kamtekar, K. T.; Bhalla, V.; Santos, J.; Bryce, M. R.; Monkman, A. P., Triplet Harvesting with 100% Efficiency by Way of Thermally Activated Delayed Fluorescence in Charge Transfer OLED Emitters. *Adv. Mater.* **2013,** *25*, 3707-3714.
35. Kim, J. U.; Park, I. S.; Chan, C.-Y.; Tanaka, M.; Tsuchiya, Y.; Nakanotani, H.; Adachi, C., Nanosecond-time-scale delayed fluorescence molecule for deep-blue OLEDs with small efficiency rolloff. *Nat. Comm.* **2020,** *11*, 1765.
36. Ishimatsu, R.; Matsunami, S.; Shizu, K.; Adachi, C.; Nakano, K.; Imato, T., Solvent Effect on Thermally Activated Delayed Fluorescence by 1,2,3,5-Tetrakis(carbazol-9-yl)-4,6-dicyanobenzene. *J. Phys. Chem. A* **2013,** *117*, 5607-5612.
37. Tanaka, H.; Shizu, K.; Miyazaki, H.; Adachi, C., Efficient green thermally activated delayed fluorescence (TADF) from a phenoxazine–triphenyltriazine (PXZ–TRZ) derivative. *Chem. Comm.* **2012,** *48*, 11392-11394.
38. Tsai, W.-L.; Huang, M.-H.; Lee, W.-K.; Hsu, Y.-J.; Pan, K.-C.; Huang, Y.-H.; Ting, H.-C.; Sarma, M.; Ho, Y.-Y.; Hu, H.-C.; Chen, C.-C.; Lee, M.-T.; Wong, K.-T.; Wu, C.-C., A versatile thermally activated delayed fluorescence emitter for both highly efficient doped and non-doped organic light emitting devices. *Chem. Comm.* **2015,** *51*, 13662-13665.
39. Zhang, Y.; Ma, H.; Wang, S.; Li, Z.; Ye, K.; Zhang, J.; Liu, Y.; Peng, Q.; Wang, Y., Supramolecular Structure-Dependent Thermally-Activated Delayed Fluorescence (TADF) Properties of Organic Polymorphs. *J. Phys. Chem. C* **2016,** *120*, 19759-19767.
40. Ma, Y.; Zhang, K.; Zhang, Y.; Song, Y.; Lin, L.; Wang, C.-K.; Fan, J., Intermolecular Interaction on Excited-State Properties of Fluoro-Substituted Thermally Activated Delayed Fluorescence Molecules with Aggregation-Induced Emimssion: A Theoretical Perspective. *Mol. Phys.* **2021,** *119*, e1862931.
41. Zhang, Y.; Ma, Y.; Zhang, K.; Song, Y.; Lin, L.; Wang, C.-K.; Fan, J., Solid-State Effect on Luminescent Properties of Thermally Activated Delayed Fluorescence Molecule with Aggregation Induced Emission: A Theoretical Perspective. *Spectrochim. Acta - A: Mol. Biomol. Spectrosc.* **2020,** *241*, 118634.
42. Niss, K.; Hecksher, T., Perspective: Searching for simplicity rather than universality in glass-forming liquids. *J. Chem. Phys.* **2018,** *149*, 230901.
43. Dyre, J. C., Colloquium: The glass transition and elastic models of glass-forming liquids. *Rev. Mod. Phys.* **2006,** *78*, 953-972.
44. Niwa, A.; Kobayashi, T.; Nagase, T.; Goushi, K.; Adachi, C.; Naito, H., Temperature dependence of photoluminescence properties in a thermally activated delayed fluorescence emitter. *Appl. Phys. Lett.* **2014,** *104*, 213303.

45. Chan, C.-Y.; Cui, L.-S.; Kim, J. U.; Nakanotani, H.; Adachi, C., Rational Molecular Design for Deep-Blue Thermally Activated Delayed Fluorescence Emitters. *Adv. Funct. Mater.* **2018,** *28*, 1706023.
46. Huang, Y.-C.; Lu, T.-C.; Huang, C.-I., Exploring the correlation between molecular conformation and UV–visible absorption spectra of two-dimensional thiophene-based conjugated polymers. *Polymer* **2013,** *54*, 6489-6499.
47. Winters, M. U.; Kärnbratt, J.; Eng, M.; Wilson, C. J.; Anderson, H. L.; Albinsson, B., Photophysics of a Butadiyne-Linked Porphyrin Dimer: Influence of Conformational Flexibility in the Ground and First Singlet Excited State. *J. Phys. Chem. C* **2007,** *111*, 7192-7199.
48. Borisenko, V.; Woolley, G. A., Reversibility of conformational switching in light-sensitive peptides. *J. Photochem. Photobiol. A* **2005,** *173*, 21-28.
49. Hoche, J.; Schulz, A.; Dietrich, L. M.; Humeniuk, A.; Stolte, M.; Schmidt, D.; Brixner, T.; Würthner, F.; Mitric, R., The origin of the solvent dependence of fluorescence quantum yields in dipolar merocyanine dyes. *Chem. Sci.* **2019,** *10*, 11013-11022.
50. Zhou, P.; Tang, Z.; Li, P.; Liu, J., Unraveling the Mechanism for Tuning the Fluorescence of Fluorescein Derivatives: The Role of the Conical Intersection and nπ* State. *J. Phys. Chem. Lett.* **2021,** *12*, 6478-6485.
51. Haynes, D. R.; Tokmakoff, A.; George, S. M., Temperature-dependent absolute fluorescence quantum yield of C60 multilayers. *Chem. Phys. Lett.* **1993,** *214*, 50-56.
52. Chen, S.; Ullah, N.; Zhao, Y.; Zhang, R., Nonradiative Excited-State Decay via Conical Intersection in Graphene Nanostructures. *ChemPhysChem* **2019,** *20*, 2754-2758.
53. Levine, B. G.; Esch, M. P.; Fales, B. S.; Hardwick, D. T.; Peng, W.-T.; Shu, Y., Conical Intersections at the Nanoscale: Molecular Ideas for Materials. *Ann. Rev. Phys. Chem.* **2019,** *70*, 21-43.
54. Olivier, Y.; Sancho-Garcia, J. C.; Muccioli, L.; D'Avino, G.; Beljonne, D., Computational Design of Thermally Activated Delayed Fluorescence Materials: The Challenges Ahead. *J. Phys. Chem. Lett.* **2018,** *9*, 6149-6163.
55. Weissenseel, S.; Drigo, N. A.; Kudriashova, L. G.; Schmid, M.; Morgenstern, T.; Lin, K.-H.; Prlj, A.; Corminboeuf, C.; Sperlich, A.; Brütting, W.; Nazeeruddin, M. K.; Dyakonov, V., Getting the Right Twist: Influence of Donor–Acceptor Dihedral Angle on Exciton Kinetics and Singlet–Triplet Gap in Deep Blue Thermally Activated Delayed Fluorescence Emitter. *J. Phys. Chem. C* **2019,** *123*, 27778-27784.
56. Turro, N. J., *Modern Molecular Photochemistry*. University Science Books: California, 1991; p 628.
57. Würth, C.; Geißler, D.; Behnke, T.; Kaiser, M.; Resch-Genger, U., Critical review of the determination of photoluminescence quantum yields of luminescent reporters. *Anal. Bioanal. Chem.* **2015,** *407*, 59-78.
58. Debye, P., Dielectric Properties of Pure Liquids. *Chem. Rev.* **1936,** *19*, 171-182.
59. Frohlich, H., *Theory of Dielectrics*. Oxford Univ. Press: 1949; p 187.
60. Lechner, M. D., *Static Dielectric Constants of Pure Liquids and Binary Mixtures: Supplement to IV/6*. Springer-Verlag: Berlin, 2008; p 203.
61. Metz, D. J.; Glines, A., Density, Viscosity, and Dielectric Constant of Tetrahydrofuran between -78 and 30 Degree. *J. Phys. Chem.* **1967,** *71*, 1158.
62. Bagchi, B.; Chandra, A., Dielectric Relaxation in Dipolar Liquids: Route to Debye Behavior via Translational Diffusion. *Phys. Rev. Lett.* **1990,** *64*, 455-458.

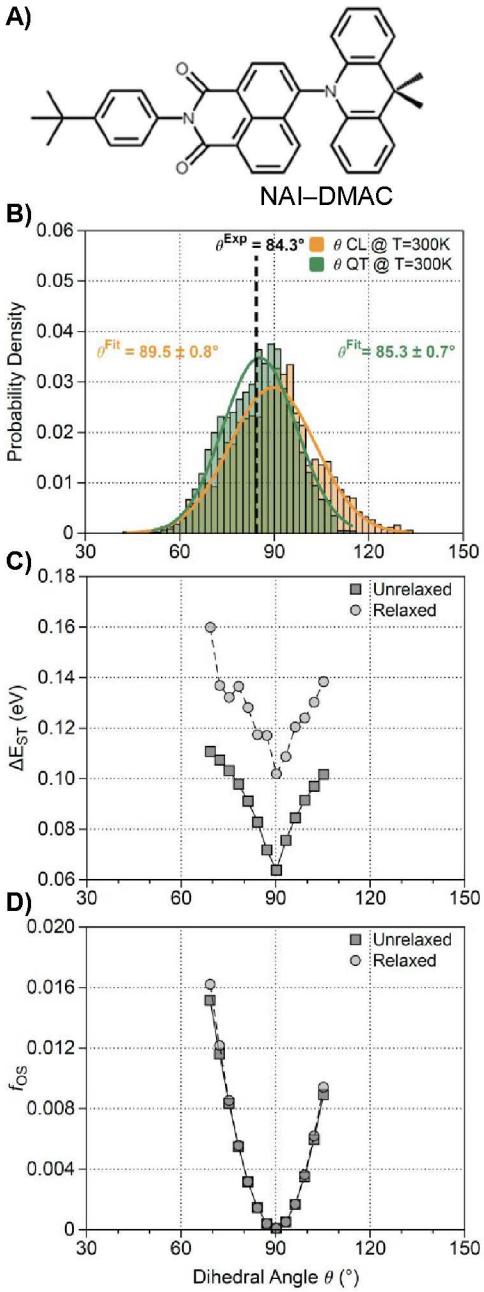

Figure 1. A) Structure of NAI-DMAC. **B)** Probability distribution of the dihedral angle between the NAI and DMAC units for isolated molecules in the gas phase at 300K from first principles molecular dynamics simulations. Values for the **C)** singlet-triplet energy splitting (ΔE_{ST}) and **D)** oscillator strength (f_{os}) of the HOMO-LUMO transition as a function of the dihedral angle between NAI and DMAC computed at 0 K. The points in both plots labeled as Unrelaxed were computed by only allowing the dihedral angle to vary. The points labeled Relaxed in both plots were computed by allowing full geometric optimization of the molecule at each angle. Adapted from Reference 17 and used with permission. Copyright Royal Society of Chemistry 2022. **DOI**: 10.1039/d2cp01147f

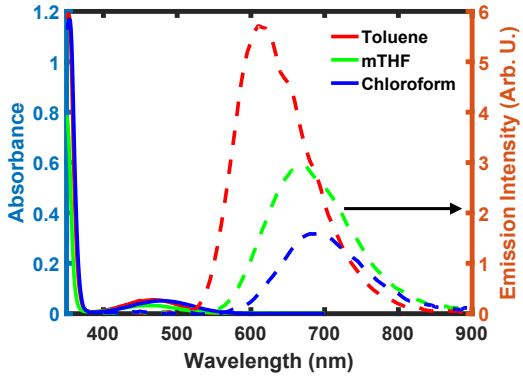

Figure 2. The optical absorption spectra of NAI-DMAC dissolved in toluene, mTHF, and chloroform are represented as solid curves. The transition around 350 nm is due to a π-π* transition localized to the NAI unit, while the feature at approximately 470 nm arises from an n-π* transition with significant charge transfer character. The fluorescence spectra of NAI-DMAC in the same series of solvents of increasing polarity appear as the dashed curves. The peak of the emission spectra shifts to longer wavelengths as the polarity of the solvent increases.

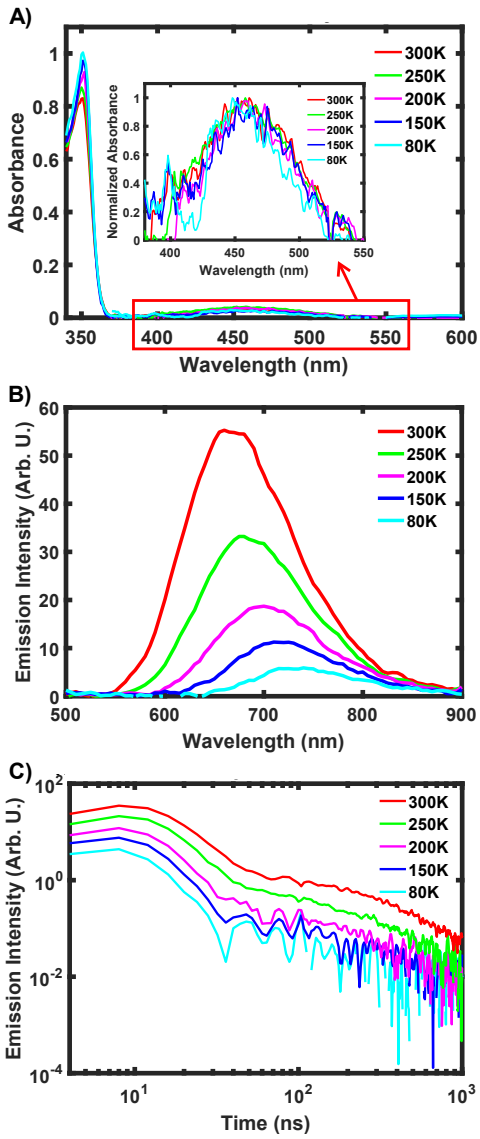

Figure 3. A) Optical absorption spectra of NAI-DMAC in mTHF measured at a range of temperatures. The inset shows an expanded view of the n-π* transition indicating little change in shape or central wavelength with temperature. **B)** Unnormalized time-integrated PL spectra of NAI-DMAC measured in mTHF at a range of temperatures following 355 nm excitation. The spectra exhibit a marked reduction of the emission quantum yield at lower temperatures. **C)** Unnormalized TRPL kinetics of NAI-DMAC measured in mTHF at a range of temperatures also following 355 nm excitation. The amplitude changes of the kinetics following quantitatively the changes of the PL spectra.

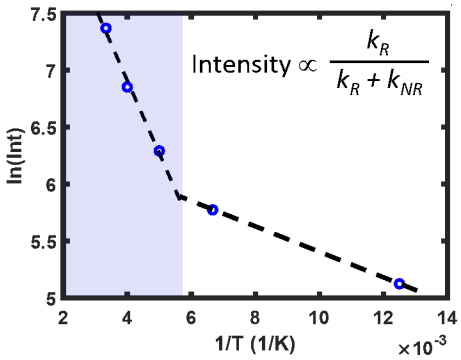

Figure 4. Plot of the logarithm of the integrated amplitude of the prompt PL component of NAI-DMAC in mTHF following 355 nm versus the inverse temperature at which the measurements were made. The amplitudes were obtained by integrating the emission from 500-900 nm and from 8-12 ns. The knee in the temperature dependence corresponds to the abrupt change in self-diffusion dynamics of mTHF at the glass transition as described in Reference 26.